IEEE Access
Multidisciplinary | Rapid Review | Open Access Journal

Received 8 January 2024, accepted 14 January 2024, date of publication 5 February 2024, date of current version 9 February 2024.

Digital Object Identifier 10.1109/ACCESS.2024.3357537

RESEARCH ARTICLE

The Empirical Analysis, Mathematical Modeling, and Advanced Control Strategies for Buck Converter

ASAD ULLAH[1], SANAM SHAHLA RIZVI[2], AMNA KHATOON[3], AND SE JIN KWON[4], (Member, IEEE)

[1]School of Information Engineering, Xi'an Eurasia University, Xi'an, Shaanxi 710065, China
[2]Raptor Interactive (Pty) Ltd., Centurion 0157, South Africa
[3]School of Information Engineering, Chang'an University, Xi'an, Shaanxi 710064, China
[4]Department of AI Software, Kangwon National University, Samcheok-si 25913, South Korea

Corresponding author: Se Jin Kwon (sjkwon@kangwon.ac.kr)

This work was supported by the Basic Science Research Program through the National Research Foundation of Korea (NRF) funded by the Ministry of Education under Grant RS-2023-00244091.

ABSTRACT The DC-DC converters are essential in power electronics as they maintain a stable output voltage even when there are changes in input voltage and load current. This study introduces an advanced Proportional-Derivative (PD) compensator for buck converters. The compensator enhances stability and transient responsiveness by employing a unique modulation technique that has not been previously applied in this context. The proposed method entails applying an input of 28 volts, which yields an output amplification of 15 volts, even in the presence of interference. The small signal transfer function of the buck converter is meticulously derived, considering the converter's dynamic behavior to achieve exceptional results. The transfer function comprehensively explains the intricate relationship between the input and output voltages, providing the theoretical basis for our distinctive control approach. The MATLAB code accurately generates the Bode diagram of the buck converter by employing the small signal transfer function. The graph illustrates the frequency response of the converter, a crucial factor in enhancing the stability and quality of the output voltage. The proposed research is substantiated by mathematical data shown through several simulated figures, distinguishing it from conventional methodologies. The implemented research achieves the maximum efficiency exceeding 95% with a minimum ripple factor.

INDEX TERMS Buck converter, compensator, MATLAB/simulink, small signal transfer function.

I. INTRODUCTION

There was a historical revolution in 1964, and after that revolution, a boost was given to the use of electronic equipment like batteries, motors, etc [1]. However, the lifetime or load time of the batteries is consistently kept under pressure to be solved, so the method of recovery of this issue is a DC-DC converter between the batteries & load supplied [2]. It is known that DC-DC converters give a fast-dynamic response, highly efficient output, and the best control of smooth acceleration. Researchers have proposed various innovative topologies for non-isolated DC-DC converters [3]. It is essential to consider the advantages and disadvantages of each topology when selecting the most suitable one for a specific application. The design process should consider isolation requirements, directionality (unidirectional or bidirectional), voltage or current feed, and minimum-phase characteristics [4]. Besides these, switching characteristics (hard or soft switched) must be considered [5]. Using a DC/DC converter, the research proposed the average switching cycle of the predicted output voltage [6]. Another research uses the DC/DC converter with low-frequency components but excludes the ripples of the switching frequency [7]. But practically, these ripples or waveforms are abundant and must be considered [8]. This research introduces a better way to control buck converters using a Proportional-Derivative (PD)

The associate editor coordinating the review of this manuscript and approving it for publication was Jiann-Jong Chen.

compensator. It makes the system more stable and responsive compared to the usual method. The study also looks at how a connected inductor and a DC-DC boost converter can work better with a steady input, and it suggests a significant change in how we control the system. An innovative Proportional Derivative compensator (PD) is introduced, showing a better and more stable response than a conventional buck converter. Important modification is done to get better performance using this PD compensator for a continuous input current [9]. The buck-boost converter is simple in design, and it is simple to adjust its functionality. So these features make them a hot choice to be selected as a DC-DC converter [10]. The converters, such as the buck-boost converter, can operate in two distinct modes: discontinuous conduction mode (DCM) and continuous conduction mode (CCM) [11].

Each approach has distinct benefits and drawbacks, depending on the specific application context. CCM is always above zero in a switching period without interrupting current, while DCM is mostly zero while switching off [12]. Each method's operation depends on the purpose because both have drawbacks and benefits where they're supposed to be applied [13]. Despite these challenges, the proposed study demonstrates an exceptional control system for a buck converter using MATLAB/Simulink. The focus lies on open-loop control, specifically regarding a variable load and unadjusted loop gains, among other contributing aspects. The goal is to maintain a stable output voltage despite input voltage variations and load current variations [14]. Typically, this is achieved by utilizing sophisticated switching mechanisms often used in various applications, such as aircraft and personal computers [15]. Many applications and software are available to process different electrical and electronic experiment, their simulation, and implementation on a software base. Like MATLAB, Math Works SimPowerSys. The selection and processing directly depend on the project's requirements. In the implemented research experiment, MATLAB/Simulink controls the buck converter, keeping accuracy on priority, which has been achieved. In the performed research work the aim of stability and transient response is gained. The implemented research has a balanced converter and compensator to maintain system stability and transient response to avoid overshoot, ringing, or slow response. As multi resistances like operating conditions, temperature, and manufacturing variations was a creating difficulties to perform the proposed research but it was tackled in a systematic way. The buck converter can exhibit nonlinear behavior, especially during transient conditions or when operating at the boundary of its design specifications [16]. The main problem to be overcome during the performance of the research using buck converter is its efficiency, to have minimum ripple variation in the output voltage caused by the switching action. One critical problem to tackle is a control system with minimum noise.

The buck converter is designed to perform well under uncertain operating conditions characterized by load variations and disturbances [17]. It aims to achieve efficient and stable voltage regulation. The proposed research demonstrates that the buck converter achieves a maximum efficiency exceeding 95% and maintains a low output voltage ripple factor of 0.01. This indicates the converter can deliver a stable power supply despite load variations and disturbances. The main points that make the proposed algorithm robust and innovative are:

- The proposed method introduces a new control approach that utilizes the derivative of the output error instead of the traditional LESO concept. This enhancement aims to enhance the observer's cognitive capacity to handle information and enhance the precision of their observations.
- In the proposed research, MOSFET is employed instead of an ordinary diode in the DC buck converter, making it possible to modify the duty cycle to produce proportional alterations in the output voltage. This is validated using the simulation and computations.
- The experimental findings are promising, indicating that the proposed converter achieves a maximum efficiency above 95% while maintaining a negligible output voltage ripple factor of 0.01. This signifies that the converter can deliver a stable power output despite load variations and interruptions.
- An adaptive controller is introduced for switching modes during the experiment. This aims to ensure asymptotic stability with voltage sources of DC-DC converters at both ends, effectively addressing the transition issue.
- The detailed mathematical equations are presented to validate the proposed research work numeric results and a comprehensive switching model, offering a detailed analysis of the proposed approach.
- The innovative converter design leads to low voltage stress on semiconductors, resulting in reduced on-state resistance for power switches and improved overall efficiency.

The research is technically sound as it uses a buck converter to maintain a steady-state output voltage irrespective of input voltage change or output load. The paper presents a small signal transfer function and uses MATLAB programming to analyze the converter's frequency response and enhance the stability and quality of the output voltage. The effectiveness of the control design is demonstrated through simulation results. Due to these nonlinearities, a PD compensator that works well across various operating conditions is challenging. The PD compensator responds effectively to reject noise and disturbances in the proposed algorithm. Switching frequency and tolerance is also pivotal in the research work. The report is structured into sections with explicit titles and subheadings, providing a thorough synopsis of the study's criteria. The given parameters include an input voltage of 28V, an output voltage of 15V, an inductor with a capacitance of 50μF, a capacitor with a capacitance of 100μF, a resistor with a resistance of 3Ω, a switching frequency of 100Khz, and a

reference voltage of 5V. This research significantly enhances the field of power electronics by establishing a novel benchmark for designing and regulating DC-DC converters through a comprehensive and unique methodology. The paper is arranged as an introduction in section I. In section II, the literature review has been discussed. Section III presents the modeling along with compensated and uncompensated loop gain. This section also has details of numerical implantations. Section IV presents the simulation and their experimental results with deep analysis, and a conclusion is at the end of section V.

II. LITERATURE REVIEW

The life span of the mobile phone battery is less than that of the mobile phone. This is because customers may need to replace their batteries during the life of their phone, or they may want to have an extra battery for situations when they cannot charge their phone [18]. Consumers have little pressure to upgrade their batteries unless they fail or need a larger battery [19]. Regarding bidirectional DC-DC converters, they can charge and discharge batteries and connect them to the D.C. microgrid to effectively utilize distributed power sources [20]. However, these converters are nonlinear discrete systems with uncertain and time-varying parameters. When sudden changes occur in loads or input voltage, the output voltage can experience large drops, large-scale oscillations, long adjustment times, significant steady-state static errors, etc. [21]. If the system's input voltage or load changes significantly, the converter will show nonlinear severe characteristics. Furthermore, the system topology can change due to the bidirectional power flow, making the converter system exhibit dynamic variable structure characteristics [22].

The SEPIC, Cuk, and Zeta converters are part of the DC-DC converters buck-boost family [23]. They are known for their ability to step up or down the output voltage, making them suitable for voltage conversion applications. Unlike traditional buck or boost converters, these converters can combine both step-up and step-down capabilities. Different categories are in buck converters incorporating elements like capacitors and inductors [24]. These elements can solve complex difficulties by improving the control methods regarding voltage regulations [25]. Boost, SEPIC, Cuk, and Zeta converters are extensively used to gain reliability, efficiency, lightweight step-up, and compact DC/DC converters [26]. A research study proposed a two-phase interleaved boost converter [27]. Another Buck-boost converters are also known as the basic DC-DC converters in the field of renewable energy [28]. Initially, in electric vehicles, the DC-DC converter is used in [29]. For step-up and step-down, these converters play very important roles [30]. The SEPIC, Cuk, and Zeta converters lay in the buck-boost families used for voltage steps up and down [31]. The presence of two inductors in these converters can lead to multiple discontinuous conduction modes under certain conditions [32].

When it comes to controlling DC-DC converters, there are different approaches available. Linear controllers, such as proportional-integral-derivative (PID) controllers, are straightforward to implement but may lack robustness and struggle with external disturbances, settling time, or response time [33]. Nonlinear control techniques have been developed to overcome multiple limitations [34]. These include direct pole placement, fuzzy control, model predictive control, sliding mode control, and feedback linearization [35]. Each of these techniques offers unique possibilities for achieving the desired control performance. The article discusses different strategies and techniques for controlling DC/DC converters in power applications. One common strategy is variable-duty-cycle control, which involves modifying the voltage loop of a control system to reduce distortion in the inductor current [36]. The minimum distortion can be achieved by feedforward input voltage [37]. But for the same kind of results, there are also square-root operations, synthesizing of harmonic components, and multiplication to be used [38]. The high-gain DC/DC converters in photo-voltaic (P.V.) cells prevail [39]. P.V. modules require a higher voltage gain than the grid voltage waveform [40]. The duty cycle and inductor current relationships are directly proportional when the transition from DCM to CCM occurs [41]. Mode change from DCM and CCM is also difficult and challenging [42]. Linear controllers like PID controllers cannot be used throughout the converter's entire operating range due to this nonlinear behavior [43]. Advanced control strategies are required to handle the transition between different modes effectively. Various approaches have been proposed, such as sliding mode control, adaptive controllers, self-tuning adaptive controllers, predictive current control, and parameter insensitive control [44]. These techniques aim to improve efficiency, reduce harmonic content, and ensure stable operation of the DC/DC converters in different modes. The comparison also includes SEPIC, the Cuk, and the Zeta converter [45]. In simpler terms, researchers have been studying different ways to control DC-DC converters to improve their efficiency and performance. The researcher [46] used the discontinuous conduction mode in a transformer coupling for a high-gain DC-DC Converter. To address multiple issues, researchers have proposed hybrid boosting converters and switched-capacitor structures that combine different advantages to enhance the converter's performance [47]. Interleaving techniques, which involve using multiple parallel channels, have also been explored. These techniques offer benefits like harmonic cancellation, improved efficiency, and increased power density [48]. Developing new converter structures and understanding different operational modes for DC-DC converter performance lies in the advanced control techniques [49]. These days, DC-DC converters are used in bulk for electric vehicles for voltage conversion and switching [50]. Not only limited electric vehicles but also aircraft, personal computers, and D.C. motor drives are using it [51]. The potential challenge in implementing adaptive control

is the complexity of the control algorithms. They are high computational devices due to complexity, robust and reliable system. Any estimated value can affect the control performance, discontinuous control actions that produce additional noise, disturbances, and tuning of sliding mode. To crack all these issues, researchers should be focused and stick to their aim. The basic target for this kind of converter at any cost is to maintain the steady-state voltage [52]. ZVS converters are very famous for their double voltage [53]. Several applications like MATLAB, MathWorks SimPowerSys, and PLECS are used to implement converters [54]. Many researchers use MATLAB/Simulink for controlling purposes under various conditions [55]. The implemented work presented here is divided into different sections and subsections. These sections cover every aspect of the buck converter, including its operation, control strategies, and challenges. A deep comparison is done with the references to enhance the implemented work comprehensively.

III. MODELLING OF BUCK CONVERTER

The buck converter is used as a step-down converter [56]. Researchers use different designs to make a robust buck converter. The main components are diodes, a transistor (mainly MOSFET), which controls the pulse-width modulation, an inductor, and a capacitor [57]. This transistor controls the rapid on and off, generating a square wave signal. During the on state, this current passes through the inductor L and stores energy in its premises of magnetic field. In the inverse process, the discharge process occurs when no current exists through L. The stored energy in the inductor's magnetic field causes the current to continue flowing through the diode and into the output C. This allows the inductor to transfer energy to the output side. The desired reference output can be gained by carefully adjusting the PWM control signal's duty cycle. The buck converter operates by periodically storing and transferring energy from the input to the output. Its ability to step down the input voltage makes it useful in applications requiring a lower voltage level, such as power supplies for electronic devices. The Figure below shows that PWM controls the injected voltage passed through the L.C. circuit.

It is known that PWM is a technique used to control the voltage supplied to devices [58]. In Figure 1 above V_{in} = is the voltage source, L is the inductor, C is the capacitor, R is the resistor, and Vo is load voltage, where PWM regulates the injected voltage that passes through the circuit. This injected voltage is given to the inductor and capacitor of the circuit and generates an alternating current (AC). The diagram shows the mechanism of the modulation of the voltage signal using a square wave signal with varying duty cycles. The duty cycle refers to when the signal is ''on'' versus ''off''. When the switch (represented by the transistor in the Figure) is on, the current flowing through the circuit increases gradually until it reaches a peak value. This process is known as inductor charging. Discharging of energy occurs when the switch is in the off state, causing the current to decrease gradually. This discharge process is called inductor discharging and is facilitated by the diode in the circuit. The time the switch is on or off can be adjusted by controlling the duty cycle of the square wave signal used to modulate the injected voltage. This, in turn, enables precise control over the energy stored in the inductor during the charging phase and the discharge rate during the discharging phase. As a result, PWM can be used to regulate the output voltage of an L.C. circuit with greater accuracy and efficiency.

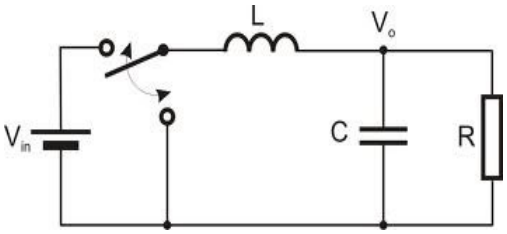

FIGURE 1. Buck converter circuit.

A. PROPORTIONAL-DERIVATIVE COMPENSATOR DESIGN

Below, equation 1 shows the transfer function of a lead proportional derivative (PD) design compensator.

$$G_c(s) = G_c o\left(\frac{1 + {}^{s}/_{\omega_z}}{1 + {}^{s}/_{\omega_p}}\right) \tag{1}$$

In the above equation 1, the cascaded compensator $G_{(s)}$ is the desired output. G_c is transfer function in s-domain. $G_c o$ is known as the direct current gain of the compensator. It indicates the value of the transfer function as ''s'' approaches zero. This complex frequency variable in the Laplace domain has both a real and an imaginary part. The nominator is known as the real, while the denominator is known as the imagery part. Where ${}^{s}/_{w_z}$ and ${}^{s}/_{w_p}$ is the lead component that may provide the desired time response. The design objective is to provide the desired crossing frequency. Once the open loop frequency is examined, the positive gain and phase contribution can be driven. In equation 2, $F^{\emptyset}_{max}$, represents the maximum force that can be exerted and the product of two other frequencies $\sqrt{f_z f_p}$. In the equation f_z represents the natural frequency of the system in the z-direction. Every system has a characteristic frequency at which it naturally oscillates or responds to external forces. The natural frequencies are influenced by mass, stiffness, and damping within the system. f_p represents the system's natural frequency in the p direction, which exhibits different natural frequencies in different directions due to its structural characteristics or design considerations.

$$F^{\emptyset}_{max} = \sqrt{f_z f_p} \tag{2}$$

Equation 2 expresses a relationship between the maximum force and the product of the natural frequencies in different directions. The $F^{\emptyset}_{max}$ is used to find the maximum force. On the left-hand side of the equation, the square root operation allows the combined effect of the two natural frequencies

on the maximum force to be considered. These variables show that each frequency and their interaction determine the external forces. Equation 3 below represents the transfer function of a PD controller. In which $G_c(s)$ represents the transfer function of the PD controller in the Laplace domain. It is a mathematical expression that relates the controller's output to its input and the Laplace variable s. G_co is the static gain of the controller. It denotes the controller's output ratio to its input at steady-state conditions. In the equation ω_z showing the frequency at which the proportional gain of the controller starts to decrease. It is the zero frequency because it corresponds to a point where the transfer function is zero. ω_p represents the frequency at which the derivative gain of the controller starts to increase. It is known as the pole frequency because it corresponds to a point where the transfer function is infinite. $1 + {}^{s}/_{\omega_z}$ a high-pass filter characteristic introduced by the proportional gain of the controller. It attenuates low-frequency signals and enhances high-frequency signals. While $1 + {}^{s}/_{\omega_p}$ does the derivative gain of the controller introduce a low-pass filter characteristic. It attenuates high-frequency signals and enhances low-frequency signals. And $\frac{\left(\frac{\omega_z+s}{\omega_z}\right)}{\left(\frac{\omega_p+s}{\omega_p}\right)}$ is the entire transfer function of the PD controller after factoring in the frequency response of both the proportional and derivative gains.

$$G_c(s) = G_co\left(\frac{1+{}^{s}/_{\omega_z}}{1+{}^{s}/_{\omega_p}}\right) = G_co\left(\frac{\left(\frac{\omega_z+s}{\omega_z}\right)}{\left(\frac{\omega_p+s}{\omega_p}\right)}\right) \tag{3}$$

The output of equation 3 is known as the transfer function. At the end of the equation, the numerator contains the zero frequency and the Laplace variable s, which introduce a high-pass filter characteristic. This means that low-frequency signals are attenuated while high-frequency signals are amplified. In comparison, the denominator contains the pole frequency and the Laplace variable s, introducing a low-pass filter characteristic to the system. This means that high-frequency signals are attenuated while low-frequency signals are amplified. The ratio of these two polynomials represents the frequency response of the entire PD controller, which includes both the proportional and derivative gains.

$$f_z = f_o\sqrt{\frac{1-sin\theta}{1+sin\theta}} \tag{4}$$

$$f_p = f_o\sqrt{\frac{1+sin\theta}{1-sin\theta}} \tag{5}$$

Equations 4 and 5 represent the relationship between frequencies with an angle θ. In equation 4, the relationship is in-between zero frequency, while equation 5 has a relationship with pole frequency over the resonant frequency f_o. Sin θ represents the sine of the angle θ, which is related to the damping ratio of the system. The equation relates the zero frequency of a system to its resonant frequency and the damping ratio. It provides a way to determine the zero frequency based on the resonant frequency and system damping.

$$f_o = 5KH_z \tag{6}$$

Resonant frequency f_o is shown in equation 6, which is the natural frequency at which the system oscillates most strongly in the absence of damping. In the proposed research, the injected value for resonant frequency is $5KH_z$, so the value can be fed to get equations 7 and 8. After putting the value and angle value into equations 4 and 5, the respective equation will be transformed into equations 7 and 8.

$$f_z = 5KH_z\sqrt{\frac{1-sin52^\circ}{1+sin52^\circ}} = 1.7KH_z \tag{7}$$

$$f_p = 5KH_z\sqrt{\frac{1+sin52^\circ}{1-sin52^\circ}} = 14.5KH_z \tag{8}$$

This section explains two things very clearly: a). Frequency injection purpose, and b). How is it purposed? Frequency injection determines the proposed research's resonant frequency and system damping by injecting a specific frequency value. The mathematics is done to derive the zero frequency and pole frequency. Where the injected value for the resonant frequency is 5 KHz, this value is used in equations 7 and 8 to calculate the actual frequency and imaginary frequency output. By substituting the values into the equations, the zero and pole frequencies are determined as 1.7 KHz and 14.5 KHz, respectively. These calculated frequencies provide insights into the system's oscillation behavior and help design the compensating transfer function. In equation 7 f_z representing the actual frequency and f_p is used for finding imaginary frequency output.

$$T_{uo} = \frac{HV}{DV_m} = 2.33 \tag{9}$$

Equation 9 shows the ultimate period of oscillation output, which is 2.33. Here in the equation V_m is variable amplitude, whether HV stands for the amplitude of the controller output. The period of oscillation is represented by T_{uo} takes time to complete one entire cycle of oscillation. DV_m is measuring amplitude, which is the difference between maximum and minimum values. In contrast, HV is the maximum and minimum amplitude controller agent.

$$G_{co} = \left(\frac{f_c}{f_o}\right)^2 \frac{1}{T_{uo}}\sqrt{\frac{f_z}{f_p}} \tag{10}$$

Here, in the equation 10, G_{co} represents the open-loop gain, f_c stands for the cut-off frequency, f_o is the resonant frequency, T_{uo} is the ultimate period of oscillation, f_z is the zero frequency, f_p is the pole frequency. The equation provides a way to calculate the open-loop gain of a system based on the cut-off frequency, resonant frequency, ultimate period of oscillation, zero frequency, and pole frequency.

$$G_{co} = \left(\frac{5kh}{1kh}\right)^2 \frac{1}{2.33}\sqrt{\frac{1.7kh}{14.5kh}} = 3.85 \tag{11}$$

$$G_{cs} = G_{co}\frac{\omega_p}{\omega_z}.\left[\frac{\omega_z + s}{\omega_p + s}\right] \tag{12}$$

$$\omega_z = 2\pi f_z = 10681.41 \tag{13}$$

$$\omega_p = 2\pi f_p = 91106.0 \tag{14}$$

In equation 11, we just put all the known values to get the desired output. The known values are driven from the equation 1 to 10. ω_z and ω_p value equals 2 into 3.14 with the product of zero frequency, which is already known by equations 7 and 8, respectively. The product of all these variables makes the output representing ω_z and ω_p. The product of these makes equations 13 and 14.

$$G_{cs} = 3.67 \times \left(\frac{91106.0}{10681.41}\right) \times \left(\frac{10681.41 + s}{91106.0 + s}\right) \tag{15}$$

$$G_{cs} = 31.3 \times \left(\frac{10681.41 + s}{91106.0 + s}\right) \tag{16}$$

A PD compensator, ensuring that the closed-loop system remains stable under all operating conditions, is a challenge. Adjusting the proportional (P) and derivative (D) gains is crucial for appropriately achieving the desired transient response without introducing instability. The equation is used in MATLAB to solve and implement with all variables known. The known variable values are substituted into the equation for computation. Besides all these mathematics, there might be some practical considerations or challenges in implementing the proposed PD compensator in real-world applications like computational requirements, control algorithm complexity, optimal proportional and derivative gains, exploring other compensators, robustness, and environmental variations. The Bode plot in MATLAB is shown in Figure 2 for visualization.

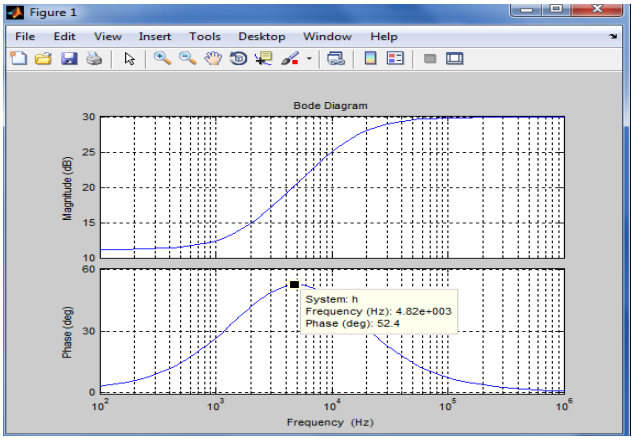

FIGURE 2. Bode plot of the original system.

A Bode plot is a graphical representation of the frequency response shown in Figure 2. The magnitude plot shows the output signal in logarithmic scale in decibels as a function of frequency. The phase plot represents the phase shift between the input and output signals at different frequencies. It illustrates the time delay for each frequency component. Understanding the phase response for the system's stability relates to the timing and synchronization of the output concerning the input signal.

B. UNCOMPENSATED LOOP GAIN

The uncompensated loop gain refers to the system's overall gain without any compensation applied. In this context, the unity compensator gain $G_{cs} = 1$ means that the compensator, a vital component in the control system, does not introduce any additional gain or attenuation to the loop. Typically, a compensator is designed to shape the frequency response of the control system to achieve desired performance characteristics such as stability, faster response, or reduced sensitivity to disturbances. However, in some cases, a unity gain compensator is used. This means the compensator's output is directly connected to the system's input without modifying the gain. A unity compensator gain in the uncompensated loop gain is used to maintain the original system gain and transfer function [59]. By setting the unity compensator gain 1 in the uncompensated loop gain, the overall system gain is preserved, allowing other compensators or feedback components to be added to the control loop without significantly changing the system's original behavior.

$$Q_o = R\sqrt{\frac{c}{L}} = 9.5 \tag{17}$$

In equation 17, Q_o represents the quality factor of a circuit, where R is the resistance, c is the capacitance, and L is the inductance. The Q factor (known as the quality factor) measures the damping characteristics of the resonant circuit. It is a parameter without any dimension that relates the system's stored energy to the dissipated energy. R is a resistance that opposes current in a circuit. Higher value-resistant devices mean high opposition, and as a result, the Q factor will decrease, creating a bearable damping response. The other main component is capacitance, which stores electrical energy in an electric field. A value capacitor will increase the capacitance of the circuit and promote a higher Q factor. As the Q factor and damp response are inversely proportional, there will be a damped response with high selectivity when there is high capacitance. There is also inductance; if the value is big enough, it will store more energy in the premises of its magnetic field, helping a more selective response through a higher Q factor. The square root of the ratio of C divided by L represents the relative balance between the energy storage capabilities of the capacitance and inductance elements within the circuit. It influences the circuit's overall sensitivity and responsiveness to frequency changes. A higher Q factor signifies a more selective and less damped response, while a lower Q factor indicates the opposite.

$$T_{u(s)} = T_{uo}\frac{1}{1 + \frac{s}{Q_o\omega_o} + \left(\frac{s}{\omega_o}\right)^2} \tag{18}$$

$$T_{u(s)} = \frac{2.33}{1 + \frac{s}{Q_o\omega_o} + \left(\frac{Q_o S}{Q_o\omega_o}\right)^2} \tag{19}$$

$$T_{u(s)} = \frac{2.33 \times Q_o^2 \omega_o^2}{Q_o^2 \omega_0^2 + Q_o \omega_o s + Q_o^2 \omega_o^2} \tag{20}$$

Equations 18, 19 and 20 $T_{u(s)}$ represent a second-order transfer function in the Laplace domain. The output of all the equations are $T_{u(s)}$, which shows the responds to an input signal in terms of its amplitude and phase characteristics. Equation 18 is the general equation, after putting the values in the equation, the new equation is equation 19, and after solving it mathematically, the equation is transformed into equation 20. In the above equations T_{uo} is used for the steady-state output when it reaches a stable condition in response to a constant input. ''s'' represents the complex frequency variable in the Laplace domain. It represents the value of the transfer function when the frequency s is zero. Essentially, it indicates the system's response to a constant DC input. The Laplace transform allows us to analyze the frequency domain, where s introduces the notion of complex frequency regarding the signal's magnitude and phase aspects. Q_o known as the damping ratio or quality factor, which relates to a resonant circuit's damping characteristics and selectivity. A higher Q_o indicates less damping and a more selective response, while a lower implies more damping and a broader response. ω_o is the natural frequency of the system, representing the frequency at which the system naturally oscillates when there is no external force applied.

$$T_{u(s)} = \frac{2.33 \times 9.5^2 \times 6283.185^2}{(9.5KH_z)^2 + 9.5KH_z \times s + 90.25s^2} \tag{21}$$

$$T_{u(s)} = \frac{2.33 \times 9.5^2 \times 6283.18^2}{9.5^2 \times 6283.18^2 + 9.5\,(6283.18)\,s + 9.5^2 s^2} \tag{22}$$

Equations 21 and 22 are the extended version of equation 18; the fundamental values are inserted in these equations, and the formula has been imposed in the proposed research work. The natural frequency plays an important role in the system's behavior and determines the rate of oscillation. The damping factor and natural frequency shown in the denominator are calculated for different input frequencies to determine the system response. It can gain the system's frequency response, stability, and transient behavior by calculating the transfer function to analyze its poles and zeros at a specific frequency. After simulating the equation, the result gained is depicted in Figure 3.

Figure 3 shows the variations in amplitude and phase when the frequency is changed at the input end. The Bode plot figure shows the stability and performance when the system transfer function is changed and at the closed-loop condition. There are two subplots, the top subplot shows the magnitude, and the phase plot is at the bottom of the Bode plot figure. The top subplot represents the logarithmic ratio between the output amplitude and frequency. The units of measurement for these parameters are decibels in Hertz (HZ). The system response is flat at the low frequency, showing that the gain is close to 0 dB. But, the system reaction becomes weak when the frequency increases until it reaches the corner frequency. At the corner frequency, the gain rapidly decreases

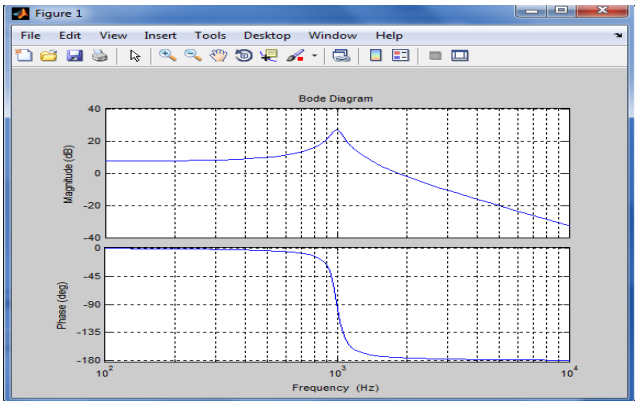

FIGURE 3. Bode plot of loop gain (uncompensated).

like a steeper slope. At this point, the system's gain starts to decrease more rapidly and makes a slope. This point is known as cut-off frequency because the maximum drop of 70.7% is noted. This is the weak point of the gain system, and the output becomes in phase with the input. At the lowest frequencies, the phase shift becomes almost zero.

The natural frequency is an important parameter in system analysis and design. It represents the frequency at which the system oscillates or responds to external forces. There are two major factors for selecting natural frequency.

- Different systems have different characteristic frequencies at which they oscillate most strongly. The system can exhibit the desired behavior by selecting a natural frequency that matches the desired response, such as fast or slow oscillations.
- Another reason for selecting a specific natural frequency is to ensure system stability. The natural frequency is related to the system's damping ratio, which determines the system's response to different input frequencies.

The natural frequency affects the system's frequency response, transient behavior, and overall performance. By choosing a natural frequency that aligns with the system's requirements, the system achieved optimal accuracy, efficiency, and responsiveness by undesirable oscillation and instability. The system's behavior justifies natural frequency to tailor and meet desired output.

C. COMPENSATED LOOP GAIN

Equation 23 represents the transfer function of a compensated system in the Laplace domain. $T_{(S)}$ denotes the output response of the compensated system in the Laplace domain. This transfer function describes how the system responds to an input signal regarding its amplitude and phase characteristics. T_{uo} stands for the steady-state output, which is the output value when the system has reached a stable condition in response to a constant input. This term scales the overall amplitude of the transfer function. G_{co} represents the compensating transfer function designed to improve the system's performance. The compensating transfer function can be

implemented using proportional integral derivative control, lead-lag compensation, or other advanced control algorithms. It introduces additional poles and zeros to shape the system's frequency response. The nominator of the equation $\left(1+{}^{s}/_{\omega_z}\right)$ represents a zero in the transfer function. A zero is a frequency at which the transfer function becomes zero, causing a change in the slope of the frequency response curve. It introduces a high-frequency boost or attenuation based on the position of the zero relative to other system parameters. The denominator $\left(1+{}^{s}/_{\omega_p}\right)$ is a pole in the transfer function. A pole is a frequency at which the transfer function becomes infinite, causing a change in the slope of the frequency response curve. It introduces a high-frequency roll-off or attenuation based on the position of the pole relative to other system parameters. $\left(1+\frac{s}{Q_o\omega_o}+\frac{s}{\omega_o}\right)^2$ represents a second-order system characterized by a quality factor Q_o and a natural frequency ω_o. It represents the response of the system to oscillatory inputs or transient disturbances. The term contains two poles and introduces damping into the system, affecting the system's response to different frequencies.

$$T_{(S)} = T_{uo}G_{co}\frac{\left(1+{}^{s}/_{\omega_z}\right)}{\left(1+{}^{s}/_{\omega_p}\right)+\left(1+\frac{s}{Q_o\omega_o}+\frac{s}{\omega_o}\right)^2} \tag{23}$$

In the above equation, the values of the ω_z, ω_p, Q_o, and ω_o are set for the desired output, where the compensating transfer function can shape the system's frequency response as desired. Equation 12 presents the transfer function G_{cs} of the increased PD compensator, which enhances the stability and transient response of the system. It allows stability, improved performance, and control over the system's transient behavior. The overall effect of the compensating transfer function is to modify the gain and phase characteristics of the system's response. The transfer function balances amplification or attenuation at different frequencies and adjusts the phase shift to achieve desired system performance. Once the parameters and values are set, the practical implemented output of the simulation curve is shown in Figure 4.

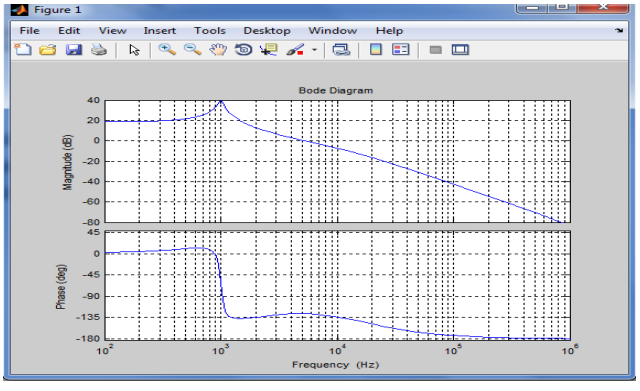

FIGURE 4. Bode plot of compensated loop gain.

A compensated loop has been gained by multiplying the original system loop gain with the uncompensated loop gain to get the overall system's compensated loop gain, which shows us that the placement of the compensator in the feedback path is valuable and increases the phase margin in Figure 4. The principal parameters of the Bode plot are explained in Figure 3. Figure 4 shows that initially, when the frequency is shallow, the gained magnitude is close to unity (0 dB), indicating that the system has a flat response, meaning it does not amplify or attenuate the input signal significantly. Till the frequency 10^3 the frequency increases, the magnitude plot starts to deviate from unity. This deviation is caused by the zeros and poles introduced by the compensating transfer function. The magnitude plot exhibits peak frequencies at this frequency, reflecting the influences. At the same frequency for the phase, the maximum indicates that the compensating transfer function introduces additional poles and zeros that lead to changes in the phase response. The presence of poles results in a phase lag, while zeros may cause a phase lead. While at low frequencies, the phase shift is close to zero degrees, indicating the system responds to changes in the input signal without significant delay.

Deep analysis and comparison between compensated and uncompensated loop gain are very important. The compensator and open loop gain make up the loop gain of the buck converter. These two components must be balanced regarding over or under-compensating for transient response and system stability. Considering the system's drawbacks, overshooting, ringing, or delayed response will occur if these components are under-compensated or over-compensated.

IV. RESULT AND DISCUSSION

The comparison between an open and closed loop of the buck converter is done in this section.

A. SIMULATION RESULTS OF AN OPEN LOOP OF THE BUCK CONVERTER

The impact of the converter's output voltage can be analyzed by switching non-ideal characteristics. This analysis will help in the deep assessments of the operations. The buck converter's operational limitation can also be pointed out with this deep analysis. Once the limitations are identified, it will be easy to use appropriate components and control mechanisms for a researcher to create innovative designs and get up-to-the-mark results. This analysis aims to reduce the negative outcomes caused by non-ideal factors. By doing this, a precise system with the required result of the system will be gained. The simulation of the buck converter done through MATLAB/Simulink uses a switch considered an idealized switch. The idealized switching means no internal drop or resistance, but it does not exist practically. So, the internal resistance should be counted for real-time performance, which makes the system more complex. During the practical implementation of switches, these internal voltage drops cause the difference between assumed and practical

output voltage. These differences impact and affect the control mechanism in the buck converter.

An open loop buck converter simulation output is shown in Figure 5. This is showing the effectiveness and impact of the non-ideal switching phenomena. It elaborates on the design and simulation process associated with the buck converter. These results clearly illustrate the practical result when internal resistance is measured. The converter performance varies in output voltage from the simulation result when the internal resistance is counted. The selection switching device will be more impactful when the switch has less internal resistance property. So, it is important to select the proper and effective switching device. The buck converter will be more efficient and practical through this selection. This improves the overall efficiency of the system.

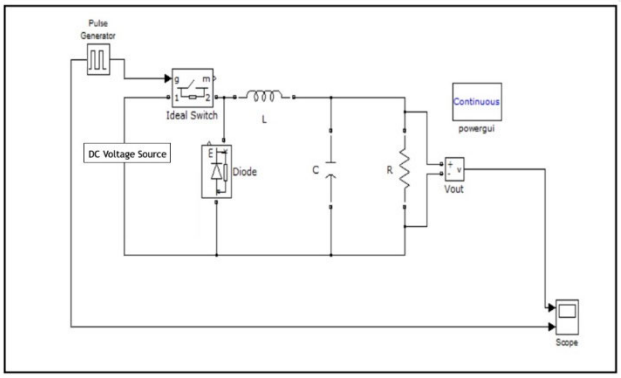

FIGURE 5. An open loop buck converter using MATLAB.

The typical open loop buck convertor output is shown in Figure 6. The generated results demonstrate the proper selection or modeling of the non-ideal features of the switch and the impact of the internal switch resistance. This deep analysis makes the experiment more perfect. By making the design more robust, the negative impact of the non-idealities will be minimized on the performance of the buck converter. Due to this simulation result of the MATLAB simulation, the buck converter assumes that in the design and optimization of the power electronics system, this is the best place as a vital tool to be placed here. Due to these ideal and non-ideal switching simulation results, the researcher can easily make a robust design by selecting the proper components. These results help in the formulation of the control strategies. Due to these deep analyses, the stability, efficiency, and accuracy will be enhanced.

B. OPEN LOOP BUCK CONVERTER WITH VARIABLE INPUT

An open-loop typical buck converter with variable input characteristics will be discussed. To find the behavior of the buck converter for a variable input, an 8V voltage pulse is generated by the pulse generator. This 8 voltage is increased to 28 by adding it with another 20V voltage generator. These voltage generators are added through an adder circuit, generating a constant voltage of 28 volts. This voltage runs the

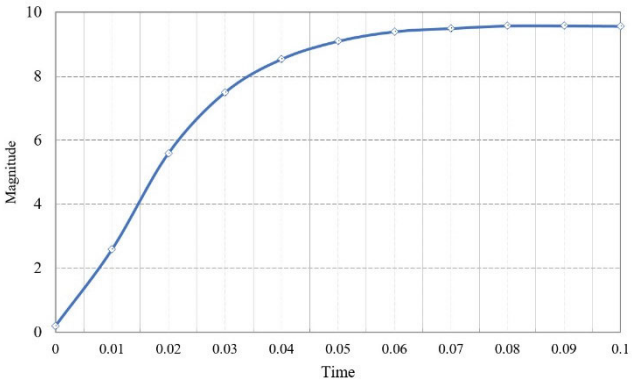

FIGURE 6. Typical of the open loop buck converter output curve.

buck converter and is known as a driving voltage. All the connections are shown in Figure 7, showing the influence of this 28-volt input on the output. To better analyze the converter's behavior, it is necessary to understand the characteristics of the input voltage.

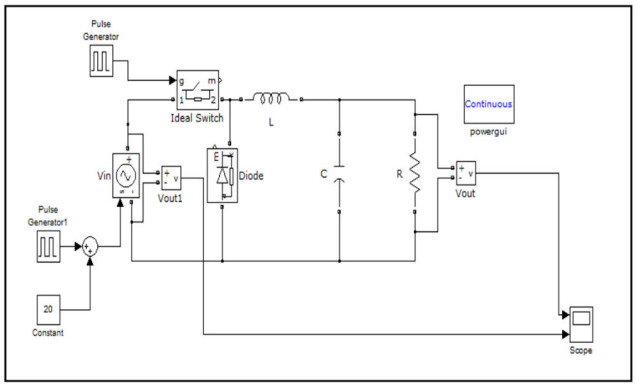

FIGURE 7. An open loop buck converter with variable input.

As the input voltage changes at the input side, the impact of these changes is highlighted, as well as the unique reaction in terms of result. Understanding, analyzing, and impacting change in the input voltage will be challenging for engineers, researchers, and scientists. They have to find the dynamic changes of the buck converter, its limitations, and the area where the result can be enhanced. Implementation is done once the change is done and the result is generated, as shown in Figure 7. The result shows the output variation when the change occurs at the input side.

Figure 8 waveform shows the efficiency and robustness of the buck converter through the output curve when variable input is given to the developed setup. There is another well-known converter known as the capacitor converter, which is used frequently in high-voltage processing. The reason for frequency use is their unique feature of utilizing three different input voltages [60]. This unique feature distinguishes it from the other capacitors explained earlier. Consequently, a thorough understanding of the unique input characteristics of the buck converter utilized in this context is of utmost importance.

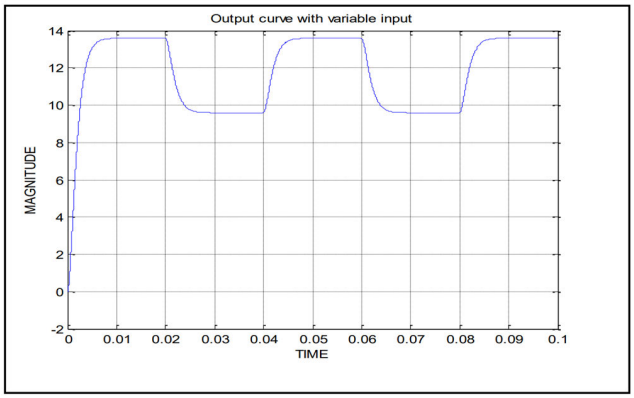

FIGURE 8. Output curve with Variable input of an open loop buck converter.

C. OPEN LOOP BUCK CONVERTER WITH VARIABLE LOAD

Different researchers are doing multiple research using buck converters. The aims are different, with different parameters and ways. For example, the researcher used linear ADRC [61]. Two resistive loads with a value of 3 ohms each are employed, and a breaker is utilized to switch between these loads. Diagrammatically, it is shown in Figure 9. Using resistive loads allows for investigating the buck converter's behavior under different load conditions. By altering the resistance value, how the converter responds and affects the output voltage, waveform can be observed. There are two major components in the resistive, known as resistive and reactive load, this resistive load. Measuring and finding this resistive load response is basic and initial to understand the performance of the converter. Based on this finding, the design and optimization process will be developed to achieve the aims in the real-world application.

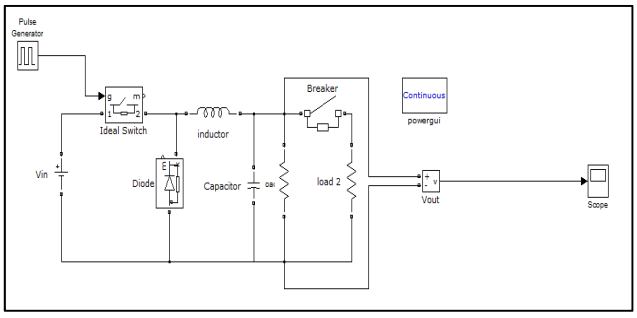

FIGURE 9. Open loop buck converter with variable output.

Figure 9 shows an open loop buck converter with variable output for the specific load characteristics. The result shows the operational behavior of the converter. A resistive load is a simplified real-world load in practical application. The practical load behavior of the buck converter is the reference point for understanding and analysis. The real-world loads demonstrate complex characteristics, including resistive and reactive elements. Utilizing the resistive load with the breaker mechanism in the implemented research work will effectively elaborate the buck converter performance. The results verify the buck converter's outclass performance in terms of stable output voltage with the variation of the load. The performance is efficient, stable, and robust for diverse operating situations.

Due to the load change, the change in the output waveform is essential. These changes in the output waveform are directly proportional to the load variation shown in Figure 10. It displays the output voltage waveform when the breaker transitions to the alternative resistive load. This waveform facilitates our comprehension of the converter's performance in the new load condition and enables us to make a direct comparison with the prior one. By comparing and analyzing the output waveforms for various loads, one can identify any disparities or similarities, allowing for the assessment of the converter's performance and its capacity to adjust to diverse load situations. The adopted design and optimization approach enables the construction of buck converters that can efficiently adjust to different load requirements found in real-world applications.

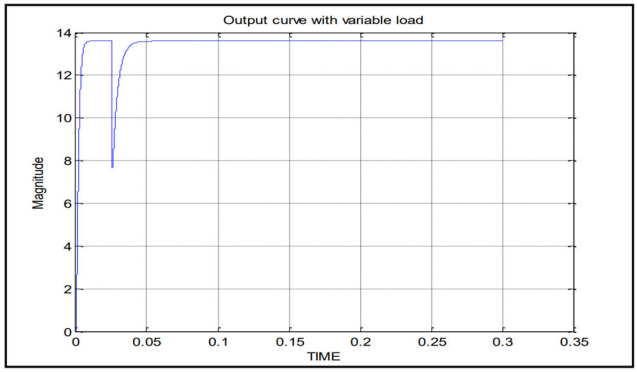

FIGURE 10. Open loop buck converter (variable load) output curve.

D. SIMULATION FOR CLOSED LOOP ON MATLAB

Extensive simulations were performed on a typical buck converter by utilizing MATLAB Simulink. Figure 11 illustrates a complex arrangement where a loop has been built, connecting the output to the input inside the open loop framework. This circuit configuration helps analyze and evaluate the converter's behavior and characteristics across numerous stages and interrelated components. It enables a thorough study of its performance and reactivity under different operational conditions. Integrating this loop into the open loop diagram enables a more thorough and precise examination of the dynamic interaction between the input and output parameters, revealing significant information about the converter's operation and possible enhancements.

Figure 12 shows the close-loop buck converter. This external source of 5K, along with the specified gain, is an input to the numerical blocks (nums and dens). The numerical blocks likely represent mathematical operations or transfer function coefficients related to the control algorithm or compensating transfer function of the converter. There are numerical blocks showing numbers and dens. The numerical blocks process the input signal from the external source. They perform

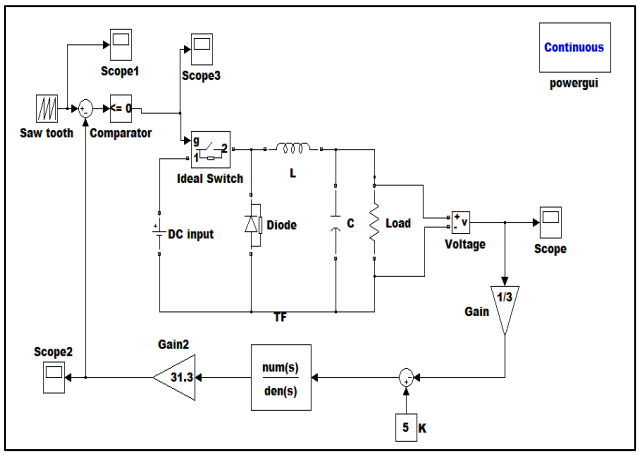

FIGURE 11. Close loop buck converter.

mathematical calculations, such as multiplication, addition, or division, to generate the desired control signal for the buck converter. There are 4 Scopes, Scope 1, Scope 2, and Scope 3, used to visualize and monitor specific signals within the circuit. Each scope is connected to different points in the circuit to analyze specific signals or variables during simulation. The purpose of each scope would depend on the intended analysis or observation in the buck converter circuit. The comparator is a fundamental component in the feedback loop of a closed-loop system. It compares two input signals and generates an output based on their differences. In this buck converter circuit, the comparator likely compares the converter's output voltage with a reference voltage to generate an error signal that controls the switching action of the ideal switch.

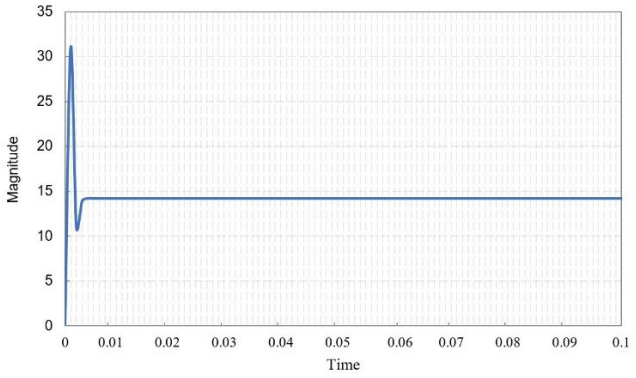

FIGURE 12. Buck converter closed loop output curve.

The ideal switch is used for the electronic switch to flow current or voltage. The output is generated once the diagram is run, as shown in Figure 13. Based on the switching operation, the comparator generates the control signal, regulating the energy transfer from the input source to the output load, as shown in Figure 14. The closed-loop buck converter utilizes an external source, numerical blocks, scopes, a comparator, a saw-tooth input, an inductor-capacitor-diode combination, a DC source, a load, and an ideal switch. Based on the comparator's feedback signal, these components regulate the buck converter's output voltage or current.

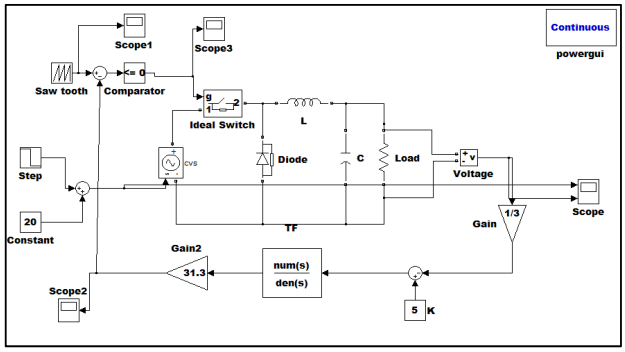

FIGURE 13. Close loop buck converter with variable input.

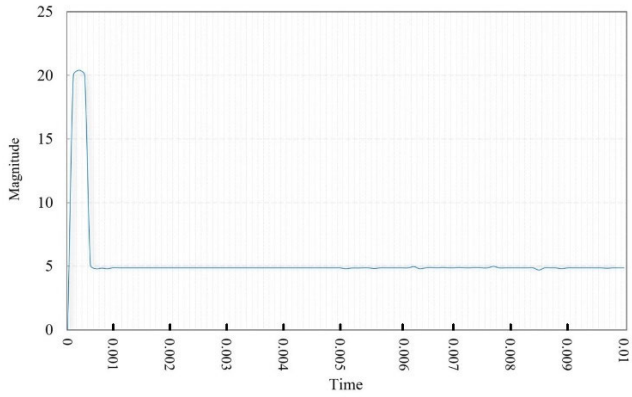

FIGURE 14. Buck Converter (for variable input) output Curve.

E. CLOSED LOOP BUCK CONVERTER WITH VARIABLE INPUT

A saw-tooth sum is shown in Figures 11 and 13; the saw-tooth waveform, along with the specified gain2, acts as an input to the comparator and Scope1. The saw-tooth waveform is often used as a ramp signal in voltage-mode control schemes to generate the control signal for the buck converter. The parallel connection of the inductor, capacitor, and diode forms the backbone of the buck converter circuit, as shown in the Figure. These components are essential for the converter's energy storage, voltage conversion, and current control. The input DC source represents the input power supply, which provides a constant voltage or current that will be converted and regulated by the buck converter. The load represents the external device that consumes power from the buck converter's output. It is connected in parallel with the output voltage and serves as the intended power recipient.

Figure 13 above shows a closed-loop buck converter circuit with variable input. The circuit likely contains similar components to those described in Figure 11, such as an external source, numerical blocks, scopes, a comparator, a saw-tooth input, an inductor-capacitor-diode combination, a DC source, a load, and an ideal switch. The only difference between

Figures 11 and 13 is that Figure 13 has external sources that are step and constant. Because of these two differences, the generated graph shown in Figure 14 shows a huge difference compared to Figure 11.

Figure 14 displays the output waveform of the buck converter when subjected to a variable input. The output curve of this Figure is smoother than the previous output waveform shown in Figure 11. This result suggests that the closed-loop buck converter circuit regulates the output voltage. The smoother output curve is due to the closed-loop control scheme's feedback mechanism. In a closed-loop system, the output signal is measured and compared to a reference value, generating an error signal. This error is important in regulating the system input or output signal. This error signal plays its role in adjusting the control signal. Whenever there is a variation in the input signal, the feedback loop is generated to regulate the output voltage or current accordingly. This makes the output waveform smooth and fine. Another method known as the compensator transfer function, also known as the control algorithm, may also improve the system's performance by adjusting the control signal. This control signal is directly proportional to the input variations.

F. CLOSED LOOP BUCK CONVERTER WITH VARIABLE LOAD

The DC-DC converter is commonly used in electronic devices to regulate the output. Voltage output in electronic devices. The closed-loop buck converter is a switch to generate or produce a steady, stable output voltage/current based on input voltage. The main target of the closed loop buck converter is to maintain this generated output stable irrespective of voltage change at the input end or load change at the other end. Figure 15 shows the closed loop buck converter with two resistive loads of 3 ohms each. The variable load is also shown in the figure below. As the load changes, the buck converter's output waveform is recorded. The output waveform shows a stable voltage output when the load is set at 3 ohms. Indicating that the buck converter is effectively regulating the output voltage despite variations in the input voltage and changes in the load. However, as the load is increased to 6 ohms, the output waveform of the buck converter changes, as shown in Figure 16. The output voltage drops, indicating that the buck converter struggles to regulate the output voltage with the increased load. This result highlights the limitations of the closed-loop buck converter when subjected to a variable load.

The implemented research work is very sound in terms of implementation as Figures 10, 11, 14, and 15 show the Open loop buck converter (variable load) output curve, Close loop buck converter, Buck Converter (for variable input) output curve, and Closed-loop Buck converter with variable load. These experimental results provide insights into the behavior and performance of the buck converter under different conditions, showcasing its stability and adaptability. Besides these, there are so many figures showing the result. These results are enhancing the quality of research work.

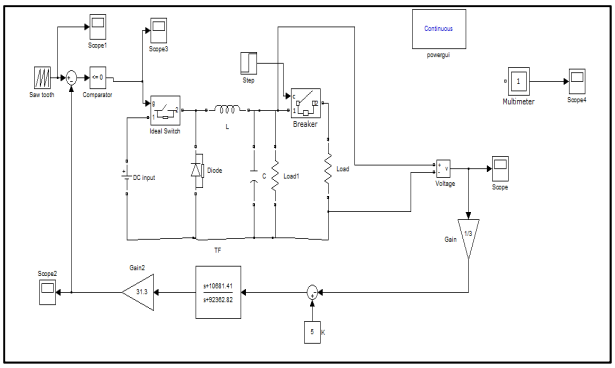

FIGURE 15. Closed-loop Buck Converter with variable load.

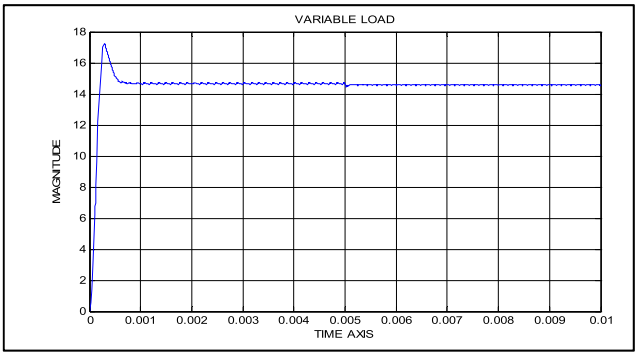

FIGURE 16. Closed-loop with variable load Output curve.

Figure 16 shows that the closed-loop buck converter regulates electronic device output voltage or current. The aim of using a buck converter is stability and making the design reliable while operating the system, so selecting the proper components is critical. Selecting appropriate components and controlling the operating system will be easy. Appropriate components will minimize the effect of change in load and voltage/current drop.

V. COMPARISON BETWEEN OPEN AND CLOSED LOOP WITH EXISTING RESEARCH WORK

Section V shows the output characteristics of an open and closed loop with variable input and output in a converter. The implemented research and results shown in different figures can be analyzed and compared. As in an earlier discussion, it is known that there is no feedback control mechanism in an open loop, due to which more ripples are generated making the output curves less steady [62]. In the absence of a feedback control mechanism, the open loop buck converter is unsuitable for input variations and changes in load. So, the overall performance or output curve fluctuates significantly and is less stable.

On the other hand, close loop conditions have a feedback control mechanism, making the output curve better in comparison. The close loop performance is better as it consists of a control mechanism that monitors and restores the change in output and current. This control mechanism has a feedback control system for both the variation that occurs on the input side and any change in the load. The purpose and target of

this control mechanism are to provide or maintain a more consistent output waveform.

Suppose it is compared which condition has a minimum raising time, whether an open or closed loop condition. Raise time is the time that is required for a system to reach its maximum final value. This specific value must be reached, which takes time. This raising time is vital to count during open and closed loop conditions. After implementation, the results of both conditions are compared. It will be easy to understand that the raising time of the close loop is much quicker or faster than the open loop condition. This means that the closed loop is more sensitive regarding raising time. Due to this rising time sensitivity, significant differences have been noticed when the output curves have been compared. In open loop conditions, sharp and short damping were observed. Due to sharp damping, oscillation occurs frequently, making the design unstable. The close loop condition is much more stable when the load changes with less damping and oscillation. The abrupt rise time and feedback mechanism stabilize the system and produce a steady state output waveform.

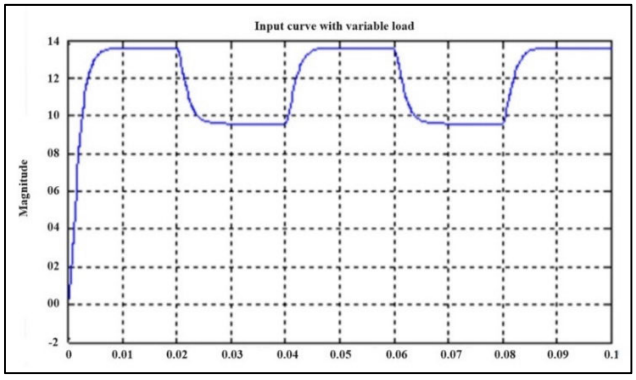

(a)

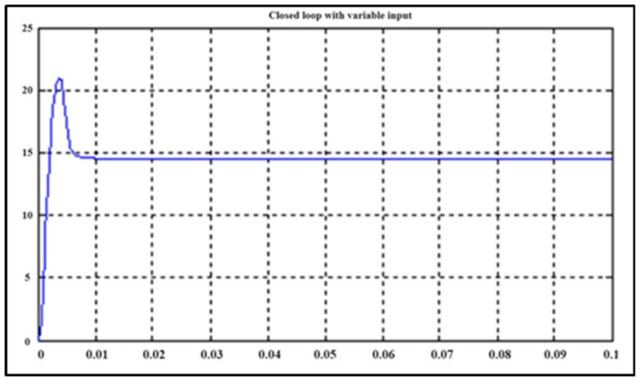

b

FIGURE 17. The output curve of open-loop (a) and closed-loop (b) buck converter with variable input.

The input variations and their variable load output curve are shown in Figures 17 and 18. The results are generated using the buck converter's open load and closed loop mechanism. The graphical representation of the output waveforms illustrates the behavior of both open- and closed-loop feedback control mechanisms. The stability and reliability have

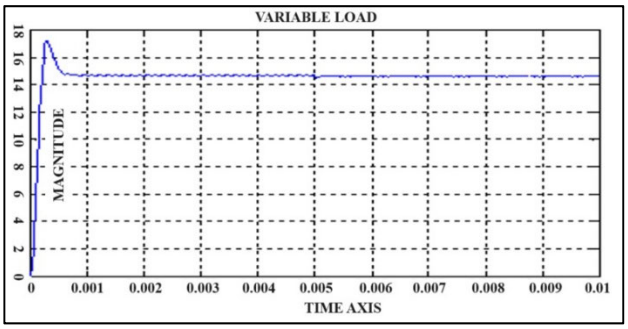

a

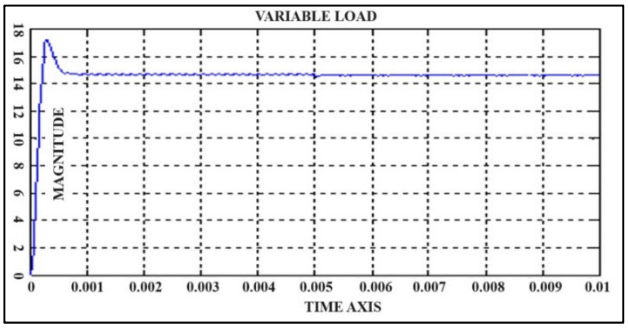

b

FIGURE 18. The output curve of open-loop (a) and closed-loop (b) buck converter with variable load.

been noticed from the output waveforms. The closed-loop configuration beats the open-loop configuration regarding overall performance and reliability. Therefore, it is essential to consider implementing a closed-loop control system when designing buck converters for applications that require robust regulation and response to input and load conditions changes. The implemented system can handle variations in criteria to ensure stable and reliable operation up to a major extent.

A study by Evren Isen uses metaheuristic optimization algorithms to compare open and closed-loop buck converters for portable electronic devices. The evaluated parameters were efficiency, transient response, and load regulation. Still, the main flaw of his research is that they only have a narrow range of load variations, which affects the applicability. The other researcher proposed using a DC-DC converter in solar photo-voltaic by Kummara Venkat Guru Raghavendra [64] and his team focused on optimizing buck converters for photo-voltaic applications, which limits its generalizability to other types of converter topologies. Houssam Eddine Ghadbane, Said Barkat, Anwar Zorig, and Dehmeche Ibrahim proposed the innovation using Robust Control Strategies for Interleaved Buck Converters. However, environmental robustness and reliability are major issues in their research work. The implemented research work could not thoroughly address the robustness and reliability of digital control techniques [65]. Scientists Moon Jiho, Lee Jaeseong, Javed Khurram, and Hong Jupyo did research work for Buck-Boost Converter for Automotive LED Matrix Headlights.

TABLE 1. The comparison table of different implemented researchers.

Implemented Research Work	Proposed Method Description	Response	Control Method	Stability	Potential	Cost effective	Assumption	Experimental Validation
[63]	Effective	Average	Stable	Stable	Low	Economical	X	Valid
[64]	Non-Roust	Fast	Stable	Stable	Low	Economical	√	Not Valid
[65]	Effective	Slow	Stable	N/A	Medium	Not	X	Not Valid
[66]	Tuning algorithm for fast transients	Slow	The current balancing method for VMC	Stable	High	Not	X	Not specified
[67]	Effective	Fast	Stable	N/A	Low	Economical	√	Valid
[68]	Strategy for wide input-output range	Fast	Frequency-domain analysis for COT control	Non-Stable	Medium	Economical	X	Not specified
[69]	Derivation of transfer functions and compensator design	Fast	Compensator design for peak current mode	Stable	Low	Not	X	Not specified
[70]	Non-Roust	Slow	Non-Stable	Stable	Low	Not	X	Valid
[71]	Practical design aspects without innovation claim	Average	Unified approach for analog compensator design	N/A	High	Economical	X	Implied but not detailed
Our Proposed Research	Design and simulation of feedback compensator for buck converter stability	Fast	PD compensator design using MATLAB/ Simulink	Stable	High	Economical	No Assumption	Detailed simulation results provided

The implemented research work was incredible as they compared traditional and predictive closed-loop control. The research showed that predictive closed-loop control significantly reduced voltage fluctuations during sudden load changes, ensuring a stable power supply to sensitive data, but due to a specific model of buck converters commonly used in data centers. This narrow focus might limit the findings' generalizability to other buck converters. Dr Smith presents his research using power-electronic buck converter modules in MVDC circuit breakers [66]. Smith and his team focused on robust control strategies for buck converters in aerospace applications. They analyzed the effects of open-loop and closed-loop control on the converter's ability to withstand harsh environmental conditions and rapid load variations. The research proposes a small signal transfer function and uses MATLAB programming to plot the Bode plot of the converter for frequency response analysis. The effectiveness of the control design is demonstrated through simulation results. The result analysis shows the steady state output voltage, showing the progress and achieving the aim. The simulation shows the empirical analysis, mathematical modeling, and advanced control strategies for a buck converter. It provides insights into maintaining the stability and quality of the output voltage in the presence of variations in input voltage and load current. Some comparative analysis is shown in Table 1 below.

The study demonstrated that closed-loop control enhanced the converter's robustness, ensuring reliable power supply in aerospace systems. There are several specific classifications of DC-DC converters mentioned in the given document. These include the SEPIC converter, the Cuk converter, the Zeta converter, and the Sheppard-Taylor topologies. These converters belong to the buck-boost families and can step up or down the voltage. They are known for their suitability in voltage conversion applications and are widely employed in various power applications, including renewable energy utilization and battery charging. The key points that make the proposed research innovative and comparative better are simplicity, cost-effectiveness, fast response and high sensitivity for an open loop and reduced sensitivity for a closed loop converter, improved regulation, and enhanced stability, with the lower transient response. Other factors making the proposed research very effective are assumptions and simplifications, scalability, accuracy, and limited environmental variations. The study focused on improving the buck converter's overall performance by incorporating the PD compensator as a feedback control mechanism. It does not specifically investigate the robustness of the PD compensator in handling sudden changes in the reference voltage or load conditions. So, no comparison is done using the sudden changes in the reference voltage. Still, it is suggested that the robustness of the PD compensator in handling sudden changes could be explored.

VI. CONCLUSION

In the study, a proportional derivative (PD) compensator is proposed and designed to enhance the performance of a simulated buck converter using Simulink. The performed research work is to implement the buck converter and observe the output as an open loop and close loop condition. The objective is to generate a steady state reference voltage as an output of the buck system. Here, the reference voltage is set as 5v, and different parameters are molted to develop the buck system.

These system parameters are input voltage (V_{in}) as 28 volts. Where the output voltage is measured in voltage is 15v. The third voltage parameter is the reference voltage, represented as V_{ref}. This voltage is kept at 5v. In other parameters, the inductor has the value of $L = 50\mu H$ (inductance in micro Henry), and the capacitor value in microfarad is $C = 500\mu F$ (capacitance). The load resistance is 3 (load resistance). After implementation, the results are compared, and it is concluded that the open loop output is less accurate and less stable because it has a lot of damping oscillation. On the other hand, the close loop buck converter is very stable, more accurate, and has an abrupt rise time.

The PD compensator is designed and added as a feedback loop for enhanced results. Two terms, proportional and derivative, are utilized to achieve the desired response. The term proportional is used to adjust the differences between the measure value and desire value, while the term derivative measures the output value for the rate of change of the error. Due to the feedback control mechanism, the close loop system uses the compensator to monitor the output voltage and keep it on the desired reference voltage. Comparing the buck converter curve with the open-loop system, the curve achieved in the closed-loop system is notably superior and more effective. This demonstrates the effectiveness of incorporating feedback control through the PD compensator in improving the buck converter's accuracy, stability, and overall performance. The performed research highlights the significance of implementing a PD compensator in designing a buck converter control system.

Several directions for future work can be explored to make the research work in buck converter control system design more robust and effective. While the proposed research utilizes a PD controller, future studies should consider experimenting with different proportional and derivative gains to determine the optimal values that yield the best response regarding transient behavior, steady-state accuracy, and stability. Researchers can identify the ideal combination of gains for improved buck converter performance by conducting extensive parameter sweeps and optimization algorithms. It would be beneficial to investigate other types of compensators beyond the PD compensator employed in the current research work. PI, PID, and MPC can be explored. These compensators may offer enhanced tracking capabilities, reduced steady-state error, and improved disturbance rejection, thereby further improving the performance of the buck converter control system. The buck converter should be tested in uncertain operating conditions characterized by load variations and disturbances.

- Automotive Industry: The proposed buck converter control system can significantly impact the automotive industry, particularly electric vehicles using LED headlights. Whenever a sudden load change occurs, the output waveform is still stable. This stability makes the overall driving less dangerous.
- Aerospace Industry: The buck converter control strategies for this industry have been discussed for better comparison. It is proved that buck converters are stable and resistive in case there is any change in the load or input voltage. So, this buck converter will positively impact if used in the aerospace industry.
- Data Centers: The robust controlling features and stability will improve the performance of the digital control techniques in data centers.
- Renewable Energy: The control feature of the proposed buck converter can also improve the efficiency in the field of renewable energy [72].

The proposed PD compensator in the buck converter was vital in energy conversion efficiency. Due to continuous monitoring and adjustment of the output voltage to the reference voltage, the closed-loop system performs well. The buck converter is more scalable as its components, control algorithms, and overall system design can handle higher power, keeping the stability, reliability, and performance well.

VII. LIMITATION AND FUTURE WORK

The proposed system is designed to use a PD compensator for linear models. So, the main drawback of the PD compensator is that it can't properly utilize nonlinearities and will not provide optimal performance. Proper tuning may be necessary to gain the desired output, but it often varies according to the specific conditions and needs of the research output. The proposed algorithm needs higher computational requirements that lead to complexity and make the algorithm challenging in real-time applications. The transient response can be carefully gained to avoid overcompensating and undercompensating. This overcompensating and undercompensating create overshooting, ringing, or slow response. The current research does not use other compensators like PI, PID, and MPC. These compensators may have the potential to enhance the performance of the buck converter.

Alternate control strategies such as adaptive control and sliding mode control can used in the future because sliding mode control employs discontinuous control actions to steer the system towards desired outputs while maintaining robustness against uncertainties and disturbances. By pursuing these future research directions, researchers can make significant strides in developing a more robust and effective buck converter control system. These efforts will contribute to the specific application domains. In the future, it will deeply elaborate on how the PD compensator inductance, capacitance, and resistance can enhance the buck converter's performance. Though, these components greatly impact the overall buck converter performance. These parameters can affect the buck converter stability, transient response, and regulation. Other compensators, such as PI, PID, and model predictive control (MPC), will have different results in comparison.

ABBREVIATION

DC	Direct Current.
V_{ref}	Reference Voltage.
V	Volt.
DCM	Discontinuous Conduction Mode.
CCM	Continuous Conduction Mode.
PID	Proportional Integral Derivative.
P.V.	Photo-voltaic.
MOSFET	Metal Oxide Semiconductor Field Effect Transistor.
Hz	Hertz.
dB	Decibel.
V_{out}	Output Voltage.
V_{in}	Input Voltage.
μ H	Inductance in Micro Henry.
μF	Capacitance in Micro Farad.
PWM	Pulse Width Modulation.
PI	Proportional Integral.
MPC	Model Predictive Control.
PID	Proportional Integral Derivative.

REFERENCES

[1] T. E. Starner and J. A. Paradiso, "Human-generated power for mobile electronics," Tech. Rep., 2004.

[2] M. F. N. Tajuddin and N. A. Rahim, "Small-signal AC modeling technique of buck converter with DSP based proportional-integral-derivative (PID) controller," in *Proc. IEEE Symp. Ind. Electron. Appl.*, vol. 2, Oct. 2009, pp. 904–909.

[3] Z. Liu, J. Du, and B. Yu, "Design method of double-boost DC/DC converter with high voltage gain for electric vehicles," *World Electr. Vehicle J.*, vol. 11, no. 4, p. 64, Oct. 2020.

[4] J. Devlin, M.-W. Chang, K. Lee, and K. Toutanova, "BERT: Pre-training of deep bidirectional transformers for language understanding," in *Proc. Conf. North Amer. Chapter Assoc. Comput. Linguistics, Hum. Lang. Technol.* Minneapolis, MI, USA: Assoc. Comput. Linguistics, vol. 1, Jun. 2019, pp. 4171–4186.

[5] B. V. Nxp, "TEA2017AAT/2 digital configurable LLC and multimode PFC controller," Tech. Rep., 2023, pp. 1–65.

[6] A. Urbonas, V. Raudonis, R. Maskeliūnas, and R. Damaševič ius, "Automated identification of wood veneer surface defects using faster region-based convolutional neural network with data augmentation and transfer learning," *Appl. Sci.*, vol. 9, no. 22, p. 4898, Nov. 2019.

[7] *UCC28065 Natural InterleavingTM Transition-Mode PFC Controller With High Light-Load Efficiency Supporting High-Frequency Switching up-to 800 kHz*, Texas Instruments, Dallas, TX, USA, 2020.

[8] C. M. Krishna, "Computationally efficient models for simulation of non-ideal DC–DC converters operating in continuous and discontinuous conduction modes," *Sadhana*, vol. 40, no. 7, pp. 2045–2072, Oct. 2015.

[9] A. Farakhor, M. Abapour, M. Sabahi, and S. G. Farkoush, "A study on an improved three-winding coupled," *Energies*, vol. 13, p. 1780, Jan. 2020.

[10] D. Murillo-Yarce, C. Restrepo, D. G. Lamar, and J. Sebastián, "A general method to study multiple discontinuous conduction modes in DC–DC converters with one transistor and its application to the versatile buck–boost converter," *IEEE Trans. Power Electron.*, vol. 37, no. 11, pp. 13030–13046, Nov. 2022.

[11] R. Manasoontorn and S. Howimanporn, "Comparison of continuous conduction mode (CCM) and discontinuous conduction mode (DCM) in omni wheel robot power supply," Tech. Rep., 2010.

[12] C. Qiao and J. Zhang, "Control of boost type converter at discontinuous conduction mode by controlling the product of inductor voltage-second," in *Proc. IEEE 36th Conf. Power Electron. Spec.*, 2005, pp. 1213–1219.

[13] E. Setiawan, "The model of continuous conduction mode and mode control in power converter," Tech. Rep., 2018.

[14] M. Forouzesh, Y. P. Siwakoti, S. A. Gorji, F. Blaabjerg, and B. Lehman, "Step-up DC–DC converters: A comprehensive review of voltage-boosting techniques, topologies, and applications," *IEEE Trans. Power Electron.*, vol. 32, no. 12, pp. 9143–9178, Dec. 2017.

[15] A. Ullah, Z. Sun, H. Rehman, S. Khan, A. Ashraf, and A. Khatoon, "Experimental and mathematical verification of permanent magnet synchronous motor using modified simulink," in *Proc. IEEE 7th Int. Conf. Smart Energy Grid Eng. (SEGE)*, Aug. 2019, pp. 86–91.

[16] M. Gheisarnejad, H. Farsizadeh, and M. H. Khooban, "A novel non-linear deep reinforcement learning controller for DC–DC power buck converters," *IEEE Trans. Ind. Electron.*, vol. 68, no. 8, pp. 6849–6858, Aug. 2021.

[17] Z. Alam, T. K. Roy, S. K. Ghosh, and M. A. Mahmud, "A hybrid non-linear voltage controller design for DC–DC buck converters," *J. Eng.*, vol. 2023, no. 10, pp. 1–15, Oct. 2023.

[18] S. Punna and U. B. Manthati, "Optimum design and analysis of a dynamic energy management scheme for HESS in renewable power generation applications," *Social Netw. Appl. Sci.*, vol. 2, no. 3, pp. 1–13, Mar. 2020.

[19] Y. Yin, J. Mao, and R. Liu, "Multivariable-feedback sliding-mode control of bidirectional DC/DC converter in DC microgrid for improved stability with dynamic constant power load," *Electronics*, vol. 11, no. 21, p. 3455, Oct. 2022.

[20] M. Gulin, "Control of a DC microgrid," Tech. Rep., 2014.

[21] L. Lv, C. Chang, Z. Zhou, and Y. Yuan, "An FPGA-based modified adaptive PID controller for DC/DC buck converters," *J. Power Electron.*, vol. 15, no. 2, pp. 346–355, Mar. 2015.

[22] S. H. A. Moghaddam, A. Ayatollahi, and A. Rahmati, "Modeling and current programmed control of a bidirectional full bridge DC–DC converter," *Energy Power Eng.*, vol. 4, no. 3, pp. 107–116, 2012.

[23] D. Murillo-Yarce, C. Restrepo, D. G. Lamar, M. M. Hernando, and J. Sebastián, "Study of multiple discontinuous conduction modes in SEPIC, Ćuk, and zeta converters," *Electronics*, vol. 11, no. 22, pp. 1–21, 2022.

[24] N. Haryani, G. Q. Lu, and S. C. Southward, "Zero voltage switching (ZVS) turn-on triangular current mode (TCM) control for AC/DC and DC/AC converters," Tech. Rep., 2019.

[25] E. Williams, "Implementation of natural switching surface control for a flyback converter," Tech. Rep., 2015.

[26] A. D. Swingler, "A new DSP controlled bi-directional DC/DC converter system for inverter/charger applications," Tech. Rep., 2003.

[27] M. A. Samad, Y. Xia, T. Manzoor, K. Mehmood, A. Saleem, A. H. Milyani, and A. A. Azhari, "Composite model predictive control for the boost converter and two-phase interleaved boost converter," *Frontiers Energy Res.*, vol. 10, pp. 1–11, Jan. 2023.

[28] N. H. Baharudin, T. M. N. T. Mansur, F. A. Hamid, R. Ali, and M. I. Misrun, "Performance analysis of DC–DC buck converter for renewable energy application," *J. Phys., Conf. Ser.*, vol. 1019, Jun. 2018, Art. no. 012020.

[29] T. Saravanakumar and R. S. Kumar, "Design, validation, and economic behavior of a three-phase interleaved step-up DC–DC converter for electric vehicle application," *Frontiers Energy Res.*, vol. 10, pp. 1–17, Jun. 2022.

[30] A. Ullah, S. Khan, and Z. Sun, "buck–boost," in *Proc. IAEAC*, Feb. 2018, pp. 54–60.

[31] J.-K. Shiau, H.-Y. Chiu, and J.-W. Sun, "Using a current controlled light-dependent resistor to bridge the control of DC/DC power converter," *Electronics*, vol. 7, no. 12, p. 447, Dec. 2018.

[32] N. T. Ajit, "Two stage interleaved boost converter design and simulation in CCM and DCM," *Int. J. Eng. Res. Technol.*, vol. 3, no. 7, pp. 847–851, 2014.

[33] M. Csizmadia and M. Kuczmann, "Extended feedback linearisation control of non-ideal DCDC buck converter in continuous-conduction mode," *Power Electron. Drives*, vol. 7, no. 1, pp. 1–8, Jan. 2022.

[34] A. M. Noman, H. S. Sheikh, A. F. Murtaza, S. Z. Almutairi, M. H. Alqahtani, and A. S. Aljumah, "Maximum power point tracking algorithm of photo-voltaic array through determination of boost converter conduction mode," *Appl. Sci.*, vol. 13, no. 14, p. 8033, Jul. 2023.

[35] Z. Li, R. Wu, T. Hu, S. Xiao, L. Zhang, and D. Zhang, "Stability analysis of an unstable slope in Chongqing based on multiple analysis methods," *Processes*, vol. 11, no. 7, p. 2178, Jul. 2023.

[36] Ü. E. Kılıç, "Design of buck converter for educational test bench," Tech. Rep., 2006.

[37] L. Wang, Q. H. Wu, W. H. Tang, Z. Y. Yu, and W. Ma, "CCM-DCM average current control for both continuous and discontinuous conduction modes boost PFC converters," in *Proc. IEEE Electr. Power Energy Conf. (EPEC)*, Oct. 2017, pp. 1–6.

[38] I. A. Kanaeva and J. A. Ivanova, "Road pavement crack detection using deep learning with synthetic data," *IOP Conf. Ser., Mater. Sci. Eng.*, vol. 1019, no. 1, Jan. 2021, Art. no. 012036.

[39] R. Yuan, S. A. Pourmousavi, W. L. Soong, G. Nguyen, and J. A. R. Liisberg, "IRMAC: Interpretable refined motifs in binary classification for smart grid applications," *Eng. Appl. Artif. Intell.*, vol. 117, Jan. 2023, Art. no. 105588.

[40] X. Yu, R. Wang, and Y. Qiao, "Research on improved high gain boost converter," in *Proc. Chin. Control Conf. (CCC)*, Jul. 2019, pp. 6504–6507.

[41] Q. Guan and Y. Zhang, "Direct charge control method for inverters in discontinuous conduction mode," *Energies*, vol. 15, no. 18, p. 6608, Sep. 2022.

[42] D. Wu, G. Calderon-Lopez, and A. J. Forsyth, "Discontinuous conduction/current mode analysis of dual interleaved buck and boost converters with interphase transformer," *IET Power Electron.*, vol. 9, no. 1, pp. 31–41, Jan. 2016.

[43] A. Ambroziak and A. Chojecki, "The PID controller optimisation module using fuzzy self-tuning PSO for air handling unit in continuous operation," *Eng. Appl. Artif. Intell.*, vol. 117, Jan. 2023, Art. no. 105485.

[44] G. Carnevale, "Distributed model predictive control for power management in small-scale off-grid energy systems," Tech. Rep., 2019.

[45] Q. He, "Modeling and simulation of boost converter with voltage feedback control," *Appl. Mech. Mater.*, vols. 668–669, pp. 482–485, Oct. 2014.

[46] K. J. Veeramraju, J. Eisen, J. L. Rovey, and J. W. Kimball, "A new discontinuous conduction mode in a transformer coupled high gain DC–DC converter," in *Proc. IEEE Appl. Power Electron. Conf. Expo. (APEC)*, Mar. 2022, pp. 237–244.

[47] M. Assaf, D. Seshsachalam, D. Chandra, and R. K. Tripathi, "DC–DC converters via MATLAB/Simulink," in *Proc. 7th WSEAS Int. Conf. Autom. Control, Modeling Simulation*, 2005, vol. 5, no. 10, pp. 906–914.

[48] Y. Wen, "Modeling and digital control of high frequency DC–DC power converters," *Converter*, vol. 10, pp. 2004–2019, Jan. 2007.

[49] Z. Lei, H. Zhou, X. Dai, W. Hu, and G.-P. Liu, "Digital twin based monitoring and control for DC–DC converters," *Nature Commun.*, vol. 14, no. 1, pp. 1–11, Sep. 2023.

[50] T. Rigaut, A. Nassiopoulos, F. Bourquin, P. Giroux, and A. Pény, "Model predictive control for energy and climate management of a subway station thermo-electrical microgrid," *Transp. Res. Proc.*, vol. 14, pp. 926–935, Jan. 2016.

[51] J. Sun, D. M. Mitchell, M. F. Greuel, P. T. Krein, and R. M. Bass, "Averaged modeling of PWM converters operating in discontinuous conduction mode," *IEEE Trans. Power Electron.*, vol. 16, no. 4, pp. 482–492, Jul. 2001.

[52] O. Flyback and C. Design, "Offline flyback converters design methodology with the L6590 family," Tech. Rep., 2001.

[53] S. Basharat, S. E. Awan, R. Akhtar, A. Hussain, S. Iqbal, S. A. Shah, and A. Yuan, "A duty cycle controlled ZVS buck converter with voltage doubler type auxiliary circuit," *Frontiers Energy Res.*, vol. 9, pp. 1–19, Feb. 2021.

[54] S. Aissani, M. Bechouat, M. Sedraoui, T. Amieur, and H. Doghmane, "Araştırma makalesi extract the transfer function of the buck converter using PLECS software," *Int. J. Adv. Natural Sci. Eng. Researches*, vol. 7, pp. 205–208, Jan. 2020.

[55] X. Niu, Z. Yang, N. Zhou, and C. Li, "A novel method for cage whirl motion capture of high-precision bearing inspired by U-Net," *Eng. Appl. Artif. Intell.*, vol. 117, Jan. 2023, Art. no. 105552.

[56] B. C. Barry, J. G. Hayes, M. G. Egan, M. S. Rylko, J. W. Maslon, and K. J. Hartnett, "CCM and DCM operation of the integrated-magnetic interleaved two-phase boost converter," in *Proc. IEEE Appl. Power Electron. Conf. Expo.*, Mar. 2014, pp. 35–42.

[57] J. Li and W. Guan, "The optical barcode detection and recognition method based on visible light communication using machine learning," *Appl. Sci.*, vol. 8, no. 12, p. 2425, Nov. 2018.

[58] H.-H. Chou, J.-Y. Chen, T.-H. Tseng, J.-Y. Yang, X. Yang, and S.-F. Wang, "A new control scheme for the buck converter," *Appl. Sci.*, vol. 13, no. 3, p. 1991, Feb. 2023.

[59] B. D. Mitchell and B. Mammano, "Designing stable control loops," in *Proc. Power Supply Design Seminar*, 2002, p. 31.

[60] X. Meng, J. Liu, G. Wang, and J. Fang, "A three-input central capacitor converter for a high-voltage PV system," *Frontiers Energy Res.*, vol. 10, pp. 1–18, Jul. 2022.

[61] W. Shen, X. Zhang, and Y. Xie, "Application and research of linear ADRC in buck converter," *J. Phys., Conf. Ser.*, vol. 2489, no. 1, May 2023, Art. no. 012034.

[62] E. Rogers and S. Power, "Understanding buck–boost power stages in switch mode power supplies," Tech. Rep., 1999.

[63] E. Isen, "Determination of different types of controller parameters using metaheuristic optimization algorithms for buck converter systems," *IEEE Access*, vol. 10, pp. 127984–127995, 2022.

[64] H. Chaoui, M. Alzayed, O. Okoye, and M. Khayamy, "Adaptive control of four-quadrant DC–DC converters in both discontinuous and continuous conduction modes," *Energies*, vol. 13, no. 16, p. 4187, Aug. 2020.

[65] N. Langenberg, S. Kimpeler, and A. Moser, "Interconnecting power-electronic buck converter modules in a novel high-power test bench for MVDC circuit breakers," *Energies*, vol. 15, no. 21, p. 7915, Oct. 2022.

[66] A. Bertolini, G. Nicollini, E. Bonizzoni, and P. Malcovati, "Practical aspects for analog compensators design in integrated DC–DC converters," *IEEE J. Emerg. Sel. Topics Power Electron.*, 2023.

[67] J. Moon, J. Lee, K. Javed, J. Hong, and J. Roh, "Concurrent current and voltage regulated buck–boost converter for automotive LED matrix headlights," *IEEE Trans. Power Electron.*, vol. 38, no. 5, pp. 6015–6023, May 2023.

[68] S. Trakuldit and C. Bunlaksananusorn, "Compensator design for a peak current mode controlled buck converter," in *Proc. 16th Int. Conf. Electr. Eng./Electron., Comput., Telecommun. Inf. Technol. (ECTI-CON)*, Jul. 2019, pp. 341–344.

[69] W.-C. Liu, C.-H. Cheng, P. P. Mercier, and C. C. Mi, "Small-signal analysis and design of constant on-time controlled buck converters with duty-cycle-independent quality factors," *IEEE Trans. Power Electron.*, 2023.

[70] A. H. Memon, R. Ali, and Z. A. Memon, "Discontinuous conduction mode buck converter with high efficiency," *3C Tecnología_Glosas Innovación Aplicadas Pyme*, vol. 2021, pp. 35–51, May 2021.

[71] T. Golla, S. Kapat, N. Chittaragi, R. A. Setty, and S. Sridharan, "Controller design and phase current balancing for fast dynamic performance in voltage mode controlled multiphase buck converters," in *Proc. IEEE Appl. Power Electron. Conf. Expo. (APEC)*, Mar. 2023, pp. 2163–2169.

[72] S. Duman, H. T. Kahraman, and M. Kati, "Economical operation of modern power grids incorporating uncertainties of renewable energy sources and load demand using the adaptive fitness-distance balance-based stochastic fractal search algorithm," *Eng. Appl. Artif. Intell.*, vol. 117, Jan. 2023, Art. no. 105501.

ASAD ULLAH received the Ph.D. degree in information engineering from Chang'an University.

He is currently an Enthusiastic and a Committed Associate Professor with the School of Information Engineering, Xi'an Eurasia University. Over the years, he have gained extensive experience teaching and conducting research, fueling his passion for academia and fostering a positive learning environment. He established a strong research foundation with Chang'an University. Additionally, he have mentored and supervised undergraduate and graduate students, providing guidance and support in their research projects and facilitating their professional growth.

SANAM SHAHLA RIZVI received the Doctor of Philosophy (Ph.D.) degree in information and communication engineering from Ajou University, South Korea. She is currently an Employee with Raptor Interactive (Pty) Ltd. She is also an experienced research and development professional with a demonstrated history of working in the computer software industry. Skilled in computer science, storage systems, databases, wireless sensor networks, and curriculum development.

AMNA KHATOON is currently pursuing the Ph.D. degree with the College of Information Engineering, Chang'an University, Xi'an, China. She is also working on remote sensing, feature extraction, and fuzzy integration. Her research interests include image processing and analysis, feature extraction, remote sensing, and algorithm analysis.

SE JIN KWON (Member, IEEE) received the B.E., M.S., and Ph.D. degrees in computer engineering from Ajou University, Republic of Korea, in 2006, 2008, and 2012, respectively. He was a Research Professor with the Department of Information and Computer Engineering, Ajou University, from 2013 to 2016. He was a Postdoctoral Researcher with the University of California at Santa Cruz, Santa Cruz, in 2016. He is currently an Associate Professor with the Department of AI Software, Kangwon National University, Republic of Korea. His research interests include non-volatile memory, storage, and large database systems.